JOURNAL OF GEOPHYSICAL RESEARCH, VOL. 95, NO. A6, PAGES 7857-7867, JUNE 1, 1990

Toroidal Standing Waves Excited by a Storm Sudden Commencement: DE 1 Observations

L. J. CAHILL, JR.,[1] N. G. LIN,[2] J. H. WAITE,[3] M. J. ENGEBRETSON,[2] AND M. SUGIURA[4]

A 74-nT sudden commencement on July 13, 1982, was observed in the magnetosphere with instruments on the Dynamics Explorer 1 satellite. Inbound, near $L = 4.5$, the satellite was located at 1524 magnetic local time and 20° magnetic latitude. The sudden commencement established a strong, east-west oscillation, with 100-s period, which was observed in the magnetic field, the electric field, and the plasma flow velocity records. There was also a compressional component of this 100-s oscillation and a rapidly damped 300-s compressional pulsation. The compressional oscillations may be evidence of cavity resonances, excited by the sudden commencement. The cavity waves may, in turn, couple to toroidal waves in field line resonance at the satellite location. In addition the sudden commencement caused the onset of waves with frequencies from 0.1 up to at least 0.5 Hz. The observations are compared with similar reports from earlier pulsations related to sudden commencements.

INTRODUCTION

It has long been observed that impulsive geomagnetic disturbances such as storm sudden commencements (SC) and sudden impulses (SI) can excite damped, quasi-sinusoidal pulsations. These pulsations are of particular interest since the time and the nature of their primary cause are quite well known in comparison to other pulsations which are usually attributed to less easily observed causes, such as the Kelvin-Helmholtz instability at the magnetopause, or to the drift-mirror instability of the storm ring current plasma. Although the abrupt rise of an SC contains a broad band of frequencies, the observed pulsations, on the ground or in the magnetosphere, usually have well-defined discrete frequencies [*Fukunishi*, 1979; *Baumjohann et al.*, 1984]. The spectra of toroidal, east-west oscillations in space have discrete, resonant peaks, and the frequencies of these peaks depend on the L value of observation. On the other hand, poloidal, radial oscillations often have spectra that are similar over a broad range of L values. In space, near but north of the equator, a westward moving field line oscillating in the fundamental mode gives an eastward deflection of B, a positive B_ϕ. In the ionosphere there is westward motion of plasma tied to the moving field line. In the lower ionosphere the positive plasma ions collide frequently with neutrals and are prevented from following the field lines while electrons are free to follow. The westward motion of electrons constitutes an eastward electrical current, and this produces, on the ground, a northward field perturbation, a positive H. The ionosphere rotates the observed pulsations counterclockwise by 90°.

The discrete toroidal oscillations (north-south on the ground) imply that the SC excite resonant toroidal oscillations of certain individual magnetic shells as is common with other non-SC pulsations [*Cahill et al.*, 1984, 1986]. The radial oscillations on the other hand must extend over a wider resonant region.

Many pulsations observed in the magnetosphere have been interpreted in terms of the theory by *Chen and Hasegawa* [1974] and by *Southwood* [1974] where surface waves on the magnetosphere create inward traveling compressional waves. These waves couple to resonant, toroidal standing waves at certain L shells where the resonant frequency of the shell matches a frequency in the spectrum of the incoming compressional waves. Resonant waves are not produced at all L shells, however. Only a set of discrete frequencies are observed. Locations of gradients in plasma density or temperature are thought to be particularly favorable to the coupling. More recently, *Kivelson and Southwood* [1985, 1986] and *Allen et al.* [1986, 1987] have proposed that impulse-stimulated magnetosphere cavity resonances could be responsible for the toroidal resonances at certain discrete frequencies. The compressional cavity resonances couple to toroidal resonance waves only at L shells where the frequencies match. Recently, observations in the outer magnetosphere with the AMPTE CCE satellite have shown continuous excitation of toroidal resonances, varying with frequency as the L value changes [*Engebretson et al.*, 1986].

Kaufmann and Walker [1974] observed an SC-caused, damped toroidal oscillation at $L = 8$ which was apparently confined to a narrow range of L shells and of longitude since it was not observed at any available ground station while the SC was observed worldwide. *Nopper et al.* [1982] used data from several geostationary satellites to show that a sudden impulse caused toroidal pulsations at several local times on the dayside of the magnetosphere. Another SI-excited pulsation event at the geostationary orbit, which had both compressional and transverse components, was observed by *Baumjohann et al.* [1984]. Toroidal waves were observed after an SC by *Wedeken et al.* [1986], but compressional waves were not observed in this case.

Several recent observations have addressed the global cavity resonances or the toroidal resonances that may be caused by them. *Kivelson et al.* [1984] observed compressional waves of period 8 min throughout the noon magnetosphere on a pass from $L = 5$ to $L = 10$. Although the wave amplitude was as large as 10 nT, no toroidal waves of similar

[1]School of Physics and Astronomy, University of Minnesota, Minneapolis.
[2]Physics Department, Augsburg College, Minneapolis, Minnesota.
[3]Department of Space Physics, Southwest Research Institute, San Antonio, Texas.
[4]Geophysical Institute, Kyoto University, Kyoto, Japan.

Paper number 90JA00020.
0148-0227/90/90JA-00020$05.00

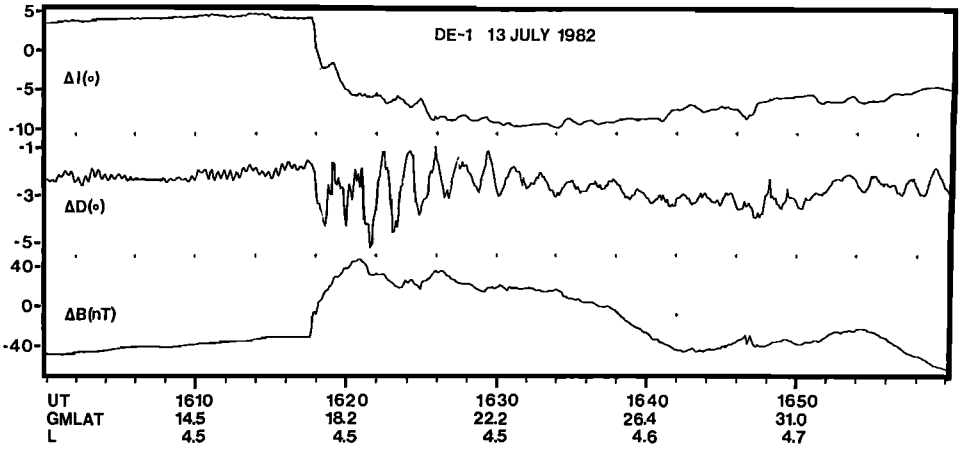

Fig. 1. Magnetic record, at the DE 1 spacecraft, of the storm sudden commencement and the resulting pulsations. The magnetic field components shown are field magnitude B, inclination angle I, and declination angle D. Note the difference in the I and D scales. The B, D, and I coordinates are described in the text. The sudden commencement is seen, just before 1618 UT, as a sudden increase in B and a sudden decrease in I. The toroidal waves are prominent in D, the east-west deflection angle. Universal time in hours, magnetic latitude in degrees, and L value in Earth radii are shown at the bottom.

period were seen. Apparently, the period did not match toroidal resonance periods in the region traversed. A large-amplitude transverse wave was observed from the ground near Tromso, Norway, by the EISCAT radar and by ground magnetometers [*Crowley et al.*, 1987]. Damping of the 10-min period waves occurred at a lower rate than the rate calculated using measured ionospheric parameters. This led to the conclusion that the wave was sustained by energy coupled from a global cavity mode. The amplitude of the cavity mode, not observed, was estimated to be 0.4 nT. *Takahashi et al.* [1988] observed compressional waves of 10-min period at 6–8 R_E. They noted the possibility that these were a global cavity resonance. Toroidal waves were also seen but with 3-min period. Perhaps low-amplitude harmonics of the 10-min compressional waves caused the toroidal waves.

The DE 1 satellite was located near the plasmapause during the wave events to be described. Since there is a strong plasma density gradient there, it seems to be a promising location for generation of waves by compressional pulses traveling in from the magnetopause. In this report we present an observation of a damped toroidal Pc 4 event which was excited by a storm sudden commencement at L = 4.5, near the plasmapause. The toroidal resonance oscillations were accompanied by weak compressional pulsations of the same period. The event was observed in data from the DE 1 magnetometer, the plasma flow instrument, and the electric field instrument, on July 13, 1982.

Observations

A small magnetic storm started on July 11, so the magnetosphere was somewhat inflated before the present event. The magnetic storm disturbance index, *Dst*, was −45 to −65 nT on July 13 before the sudden commencement, and *Kp* was 4 to 6. The storm inflation of the magnetic field at the satellite can be seen in Figure 1 where ΔB was −40 nT at 1600 UT. ΔB is the measured field magnitude minus the model magnitude [*Langel et al.*, 1980]. Inflation depresses the magnitude, near the equator, below the model value. The inclination angle is the dip angle of the field below the local horizontal plane at the satellite, positive for the downward pointing field in the northern hemisphere. Storm time inflation stretches the field lines out and increases the inclination angle, making it more positive in the northern hemisphere [*Mead and Cahill*, 1967]. The ΔI value near +4° at 1600 UT shows that the field lines are stretched out more than the model field. The declination angle measures the deflection of the field from the magnetic meridian plane, positive eastward. The pressure of the solar wind stretches the field lines toward the magnetotail [*Sugiura*, 1965]. This results in a westward, negative declination angle in the northern hemisphere for postnoon hours. Negative ΔD at 1600 UT shows that the field is stretched toward the tail more than the model field. In the remainder of the text the quantities ΔB, ΔI, and ΔD will be written as B, I, and D.

The magnetometer on Dynamics Explorer was a multirange, three-axis flux gate, with 16 vector samples per second [*Farthing et al.*, 1981]. For the data discussed here the resolution of the magnetometer was 0.02 nT, and most of the data were averaged over 6-s intervals to reduce residual effects from modulation of the measurements by the 6-s spin of the spacecraft.

The sudden commencement SC of the new magnetic storm was observed at Dynamics Explorer, at 1617:30 UT, as an abrupt increase in B. An increase by 20 nT in 10 s was followed by a slower increase to 74 nT above the starting level at 3 min after the start. After 1630 UT, B fell slowly, and on the ground, *Dst* also fell steadily after the sudden commencement, reaching a minimum, for this storm, of −338 nT near 0200 UT on July 14. The inclination angle I fell from +4° to 0° at the same time as the initial rise in B and then continued to −6° in 3 min. The decrease in I and the increase in B were due to the compression of the magnetosphere, flattening the curvature of the field lines near the equator. The angle I slowly recovered after 1630 UT as the satellite moved deeper into the magnetosphere. At the SC, D also became more negative as the field lines were forced

more toward the tail by the compression [*Mead*, 1964; *Sugiura*, 1965].

There was no continued slow change in D, however. Instead, a 100-s oscillation commenced, where the amplitude was initially 1.2°, increased to 1.6° by 1623 UT, and decreased to 0.8° by 1633 UT. The damping time was approximately 8 min. Weak pulsations of 100-s period can also be seen in I and B. The baseline of the D oscillation, the dc response of D to the compression, was 1.2° below the starting level initially, decreased to 1.7° below at 1622 UT, and returned to 0.5° below at 1629 UT. After 1630 UT the pulsations continued at a more or less constant amplitude of 0.5°–0.8°, with a shorter period, 85 s, and with several phase shifts until after 1700 UT.

There are two additional pulsations visible in Figure 1. A small-amplitude, 0.1° (equivalent to 1 nT), pulsation in D with 25-s period was present, with bursts of fluctuating amplitude, from 1600 to 1618 UT and was present sporadically after that, superimposed on the larger-amplitude pulsations. This pulsation appears to be unrelated to the sudden commencement. It is evidence of the small Pc 3 pulsations that are almost always present in this region of the magnetosphere [*Lin et al.*, 1986]. The other pulsation, in B, is weak and highly damped; one peak can be seen at 1621 UT, and a second peak is at 1626 UT. Very weak negative peaks in I can be seen at the same times, indicating that with this compressional pulsation of about 300-s period there is also a transverse poloidal component.

Plate 1 shows a spin-phase-angle-versus-time, color spectrogram of the He^+ and H^+ ion fluxes from the retarding potential mass spectrometer (RIMS) on the Dynamics Explorer satellite [*Chappell et al.*, 1981]. (Plate 1 is shown here in black and white. The color version can be found in the separate color section in this issue.) This record is from the radial (RL) head, mounted perpendicular to the eastward pointing spin axis, so the head accepts ions with velocities in the meridian plane and samples the full range of pitch angle directions as the spacecraft rotates. There are also $+Z$ and $-Z$ heads, pointing in the plus and minus spin axis directions. The count rate of the ions in the RL head is shown in a color scale representation, where red is most intense. The vertical axis, with scale on the right, shows the spin phase angle, the angle between the radial head acceptance direction, and the satellite velocity vector. At the time of these measurements the spacecraft was moving northward following the field-aligned direction, as indicated by the near alignment of the long-dashed white line (the field-aligned direction) with 0° spin phase angle (the ram or spacecraft velocity direction). Starting at 0° when the head is aimed northward in the ram (and field-aligned) direction, the head rotates with the spacecraft to +90°, pointing inward toward the Earth, then to 180°, pointing southward in the antiram (and anti-field-aligned) direction, and then to −90°, looking outward away from the Earth. The ions shown in the upper panel are singly ionized helium with energies from 0 to 50 eV, and those in the bottom panel are 0- to 50-eV H^+ ions. The apparent dominance of the He^+ ions is simply due to the relative efficiencies of detecting these ions in our detectors.

An enhanced counting rate at 0° indicates the head is scooping up ions moving in the antiram (and anti-field-aligned) directions as the satellite moves northward in its orbital motion. There are occasional indications of small He^+ count rate increases near 0° before the sudden commencement, particularly from 1600 to 1610 UT. This suggests the helium ion density is just barely large enough to produce an observable count rate from the ram velocity. The helium ion density is estimated to be about 1 cm^{-3}, and the proton density about 10 cm^{-3}. These are lower limits due to the possibility of the existence of low-energy plasma, not seen because of positive charge of the spacecraft in this low-density plasma regime. At the time of the sudden commencement there is an order of magnitude increase in the flux of singly ionized helium ions and protons. This increase may be due to an increase in the velocity or in density or both. The enhanced fluxes are seen in Plate 1 starting just before 1618 UT, where the first enhancement is seen near −90° spin phase angle when the head is looking outward. This is presumably evidence of inward motion of the ions, tied to the magnetic field lines, due to the SC compression. Subsequently, inward and outward radial motion of the ions, tied to the magnetic field lines and associated with the SC-related pulsations, produces periodic, near-100-s deflections of the direction of the ion velocity from the anti-field-aligned direction. Enhancements near −90° at 1622 UT, for example, show that the maximum inward radial bulk velocity of the ions during the pulsation is much larger than the ram velocity, 4 km/s. These pulsations in ion count rate, oscillating symmetrically about the anti-field-aligned direction, die out before 1635 UT and have a damping time of approximately 10 min.

Finally, we consider the electric field record from the University of Iowa plasma wave instrument (PWI) [*Shawhan et al.*, 1981]. The top component, E_z, shown in Figure 2 is from booms extended along the spin axis (east-west) while the $E_\perp$ and $E_\parallel$ components, perpendicular and parallel to B, are both derived from a set of booms perpendicular to the spin axis. The east-west field, E_z, is positive west; the radial field, $E_\perp$, is positive outward, and the parallel field, $E_\parallel$, is positive upward. The appropriate component to compare with the radial ion oscillations and field line motions, I, is E_z since the east-west electric field drives the radial motion. For comparison with the east-west field line motions, the $E_\perp$ radial electric field component is appropriate. The electric field records must be approached with some caution since in the low plasma density near but outside the plasmapause the measurements, particularly those from the short, spin axis booms, E_z, may be subject to errors [*Shawhan et al.*, 1981]. The sudden commencement is seen at 1617:30 UT as a westward pulse in E_z (field line motion inward) and an inward pulse in $E_\perp$ (field line motion tailward). The zero level of the z component electric field instrument probably has drifted, since the apparent continuous 10-mV/m eastward electric field from 1610 to 1617 UT is much larger than expected. Focusing on the pulsation, its zero level is at −10 mV/m between 1610 and 1630 UT. Pulsations of 100 s in period are clearly present in all three components, together with other more rapid fluctuations, mostly 25-s pulsations identified in D in Figure 1.

There are relatively large oscillations in $E_\parallel$, shown in Figure 2. Both $E_\perp$ and $E_\parallel$ are derived from the spin plane boom, with reference to the measured B vector. There is no reason to believe that $E_\parallel$ oscillations are in error, but they are larger, relative to $E_\perp$, than usually observed. There is some indication that the large $E_\parallel$ oscillations after 1620 UT are correlated with the He^+ and H^+ pulsations in count rate near 180° spin phase angle. We are searching for other

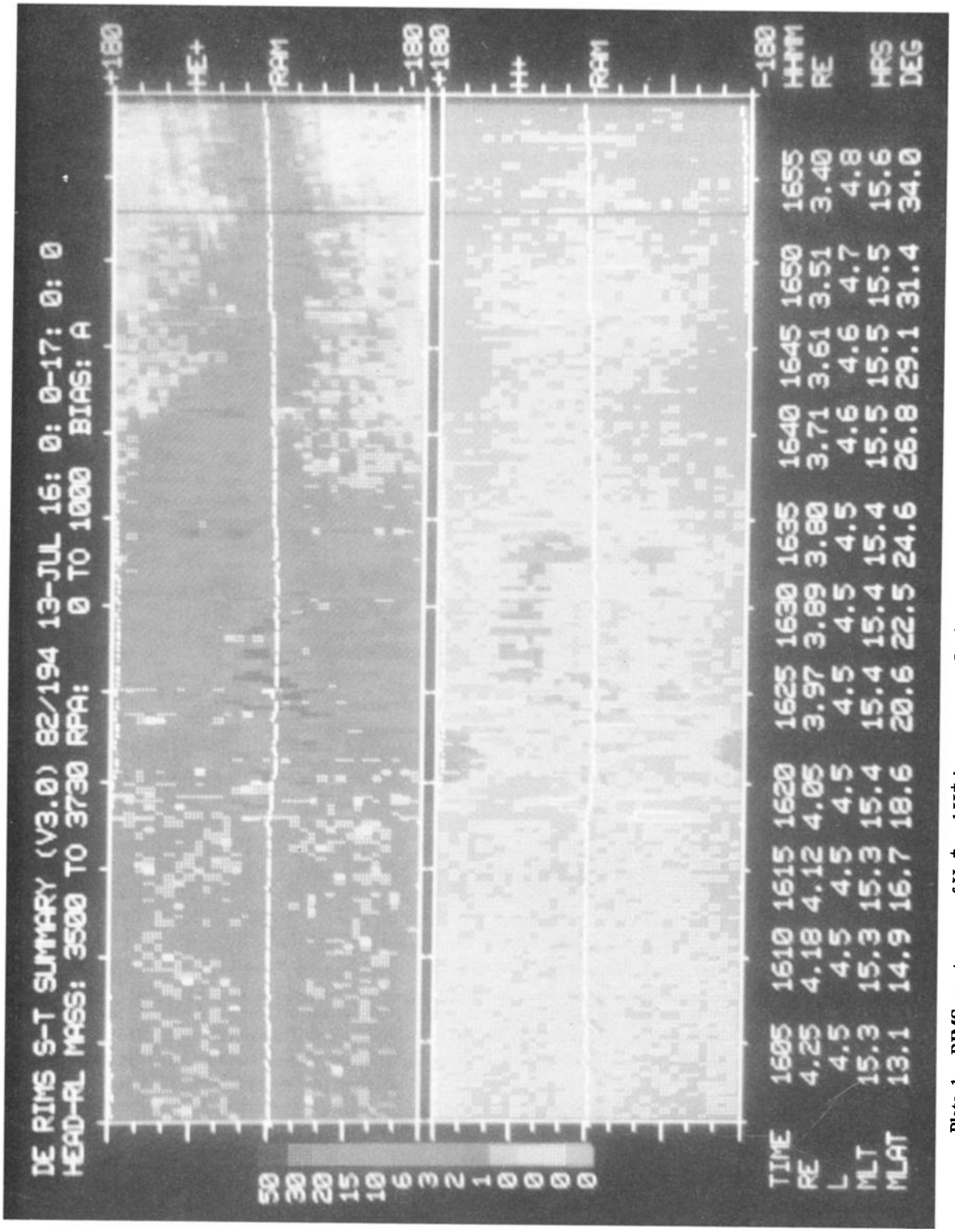

Plate 1. RIMS spectrogram of He^+ and H^+ in count rates. In the top panel the RIMS, radial head, He^+ count rate is shown (scale at left). The horizontal axis is universal time in hours; the vertical axis is the spin phase angle. The angle is described in the text; zero angle indicates the radial detector is looking in the spacecraft ram direction (the spacecraft velocity vector). Enhanced count rates at +90° indicate plasma moving out from the Earth; enhanced rates at −90° show plasma moving toward the Earth. The color version of this figure can be found in the separate color section in this issue.

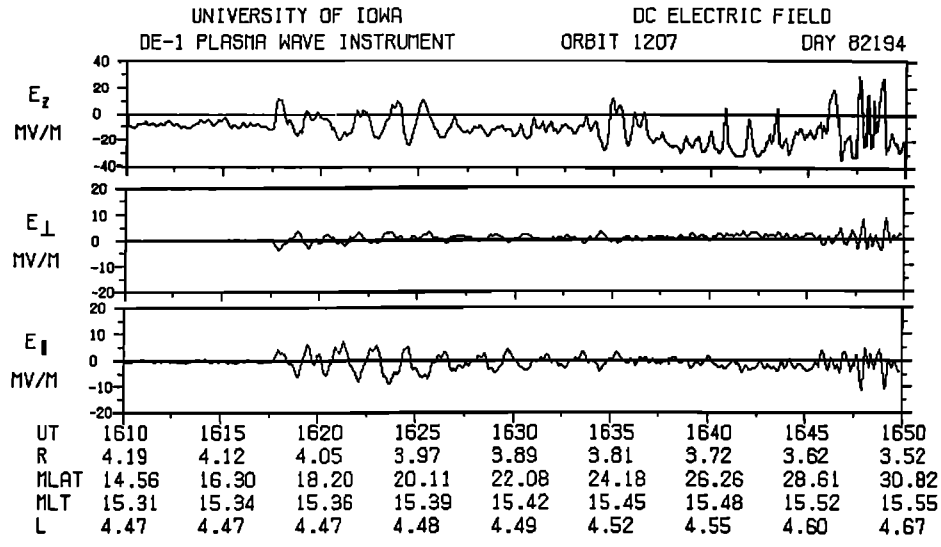

Fig. 2. Record from the electric field instrument (PWI), 1610–1650 UT. The E_z component, in millivolts per meter, is obtained from the spin axis boom, approximately east-west. The other two components are from the rotating spin plane boom. The signal from this boom is separated into components $E_\perp$, perpendicular to B, and $E_\parallel$, parallel to B. In addition to universal time in hours, the radial distance, in Earth radii; the magnetic latitude, MLAT, in degrees; the magnetic local time, MLT, in hours and tenths; and the L value in Earth radii are shown at bottom.

similar occurrences of $E_\parallel$ pulsations but will not consider the $E_\parallel$ pulsations further in this report.

In addition to the 100-s radial pulsations in ion flow, from 1617 to 1630 UT, seen in Plate 1 and discussed above, there are some other interesting ion flows and pulsations. The pulsations in count rate in Plate 1, between 90° and 180° spin phase angle, that start near 1623 UT and last until about 1630 UT are due to a counterstreaming, field-aligned flow. Together with the opposite phase pulsations between −180° and −90°, they constitute a flow up the field line, modulated by the field line oscillations, similar to the downward (or ram generated) flow with oscillations that started at 1617:30 UT. The new flow is upward (field aligned), since it first appears at 180°, and also outward, away from the Earth since the pulsations on the positive side of 180° are stronger than those on the negative side. After 1630 UT the upward flow weakens, and the pulsations are near +90° and −90° spin phase angle. The outward component of flow persists, however, since the pulsations near +90° are stronger than those near −90°. Similar but weaker flows and pulsations can be seen in the H^+ count rate until 1635 UT. After 1635 and until 1645 UT, counts are seen only in the quadrant from 0° to 90°, suggesting downward and outward flow. At 1646 UT there is a pulsation in He^+ count rates similar to the one at 1617:30 UT, together with a westward pulse in E_z (Plate 1) and an inward field line motion and field compression (Figure 1, the negative pulse in I and positive pulses in B just after 1646 UT). From 1630 to 1640 UT the relatively higher strength of the outward pulsations may be due to a radial gradient in the density of the ions. Similar effects have been seen in nonoscillating energetic ions near the magnetopause, where the plasma density is lower outside in the magnetosheath than in the magnetosphere. There, positive ions with guiding centers in higher-density layers at lower altitudes reach detectors, while traveling outward, at higher counting rates than ions from the lower-density levels traveling inward [*Lezniak and Winckler*, 1968; *Engebretson et al.*, 1983]. The higher-density boundary in the present case probably is the plasmapause.

Dynamic spectra, 0–0.5 Hz, of Figure 3 show the waves in spherical components, B_ϕ and B_θ, at frequencies up to 0.5 Hz including those above the 10-mHz resonant standing waves discussed above. The B_r spectrum, not shown, is similar to that of B_ϕ. The 10-mHz waves are seen as a dark band at the bottom of the B_ϕ spectrum. In addition there is a narrow line between 0.025 and 0.05 Hz, strongest in the B_ϕ, east-west, component that is due to the 25-s waves seen in D in Figure 1. A narrow interference line at the spin frequency, 0.16 Hz, extends across the plot, most clear before the sudden commencement. Second and third harmonic lines can also be seen. Wave activity associated with the SC extends from below 25 mHz to at least 500 mHz, although the initial SC-related waves, from 1616 to 1620 UT, are weak above 300 mHz. There is a band from 75 to 100 mHz (Pc 3), from 1616 to 1620 UT, seen on both component spectra. After 1620 UT the activity in the B_θ spectrum decreases, except for the waves below 0.025 Hz. On the other hand, the activity in B_ϕ increases, at frequencies up to 0.5 Hz. The activity above 0.1 Hz decreases after 1626 UT. From 1622 to 1625 UT there is a strong band in B_θ between 200 and 250 mHz and also activity near 50 mHz.

The sampling interval for the dynamic spectrum program is 256 points, here 256 s for one point per second data. The time location of wave events is smeared out by this process. The times shown are at the center of the 4-min interval for each vertical line of spectral power estimate. The contribution from an isolated short burst of waves will commence to appear about 2 min before the time of the wave burst and last 2 min after.

DISCUSSION

The dominant, SC-induced wave at DE 1 was the 100-s east-west oscillation. This oscillation in D can be seen

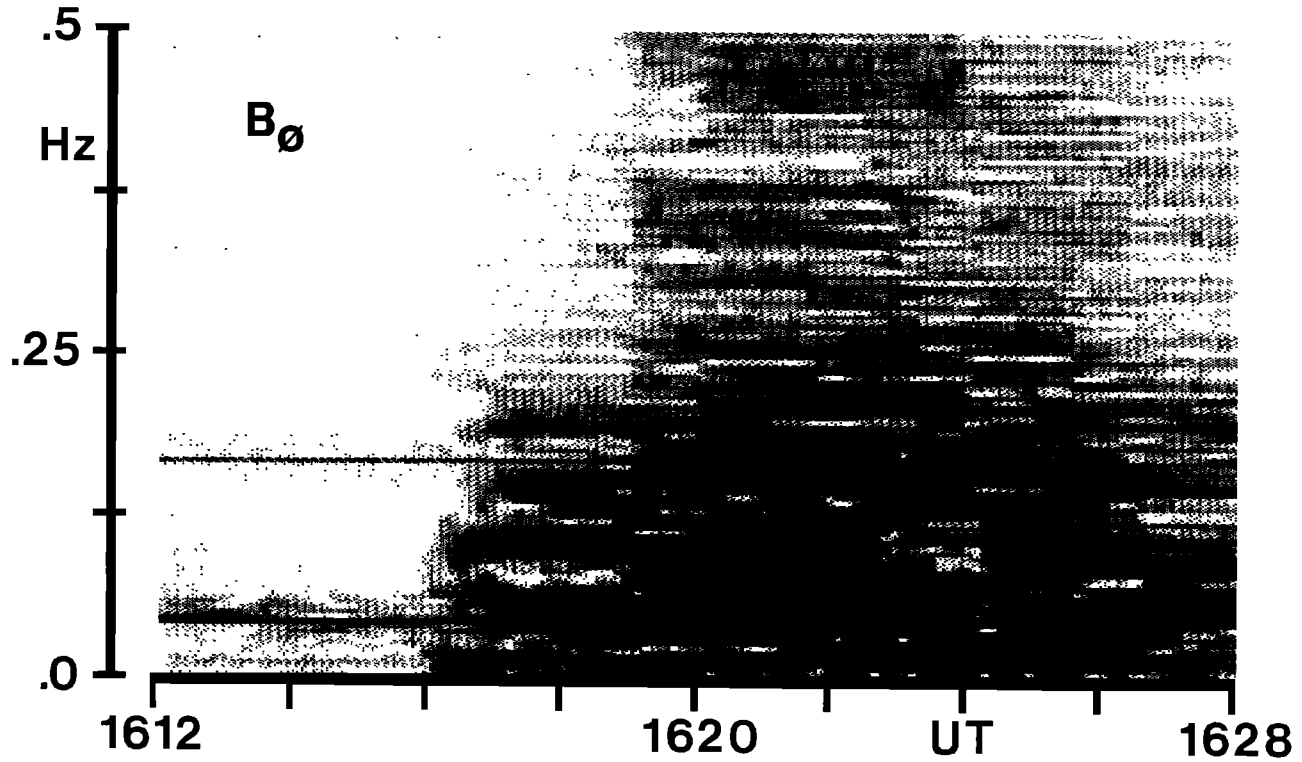

Fig. 3*a*. Dynamic fast Fourier transform spectrum, 0–500 mHz, for the B_ϕ component in spherical geomagnetic components. Each data sample, vertical spectral line, uses 256 data points at one point per second. The spectrum line is plotted at the center of the time interval.

clearly in Figure 1, with remarkably constant period and phase, from 1618 UT until after 1630 UT. When the phases of the electric and magnetic components of this toroidal pulsation are compared, it is clear that it must be a fundamental field line resonance. Although the comparison is not shown here, the associated electric field component, $E_\perp$, is at a maximum amplitude pointing outward away from the Earth when the D oscillation is crossing from negative to

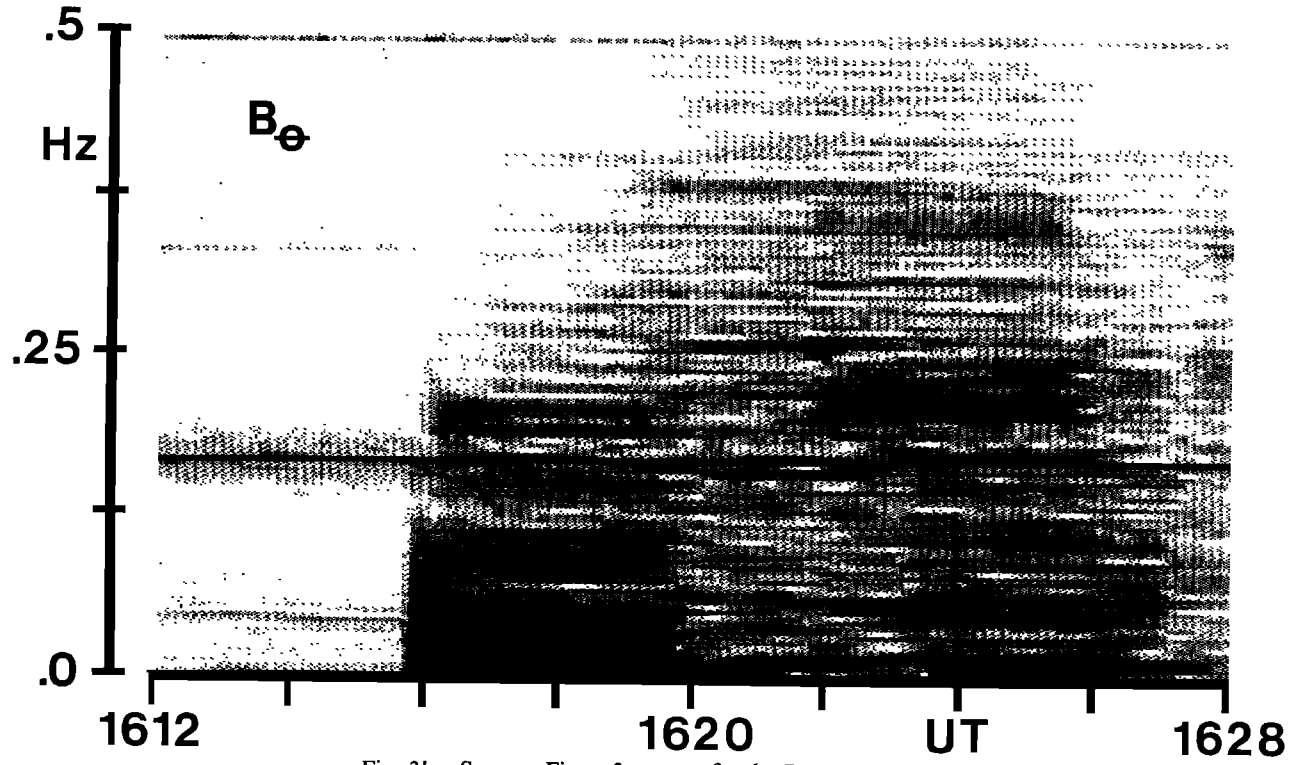

Fig. 3*b*. Same as Figure 3*a* except for the B_θ component.

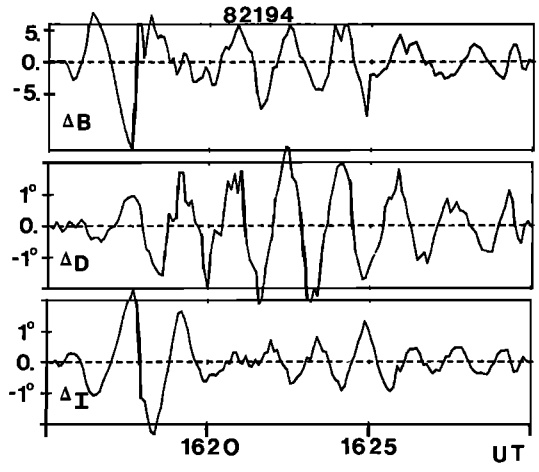

Fig. 4. A *BDI* plot of the magnetic pulsations from 1615 to 1630 UT. A 90-s sliding average has been subtracted from the data of Figure 1 in order to show the B and I pulsations more clearly.

positive, appropriate for the fundamental field line motion from east to west. At the latitude of the observations, 20° magnetic, both second and third harmonics have the opposite phase relation [*Cahill et al.*, 1984, 1986]. The velocity and amplitude of the toroidal field line motion described above may be estimated by using the measured perpendicular (approximately radial) component of E, since $v = E_\perp \times B_0/B_0^2$. $E_\perp$ is about 5 mV/m, and B_0 is about 300 nT, so $v = E/B_0 = 17$ km/s for the toroidal oscillation. We take the $E_\perp$ value from Figure 2, despite the caution about E errors outside the plasmapause. $E_\perp$ is from the long booms, and the pulsation amplitude here is similar in magnitude to values observed in earlier studies. Some of the earlier cases yielded field line and plasma speeds that were confirmed by separate determinations from the RIMS data [*Cahill et al.*, 1984; *Waite et al.*, 1986]. Also, since the toroidal amplitude $A_0 = v/\omega$, the field line moves ±270 km in the east-west direction.

In addition to the toroidal pulsations there are oscillations of similar period in B and I in Figure 1 as well as in E_z in Figure 2 and in the radial plasma flow velocity in Plate 1. Thus the toroidal pulsations are accompanied by poloidal and compressional pulsations of similar period. The compressional pulsations may be examples of the proposed cavity mode resonance compressional pulsations, in this case coupling to toroidal field line resonances of about 100-s period. In order to see the 100-s pulsations more clearly, a sliding average (120 s) was subtracted from the records of Figure 1, and the results, with expanded B and I scales, are shown in Figure 4. The D record is little changed from Figure 1, but the B and I 100-s pulsations stand out more clearly. The fluctuations before 1617:30 UT, the SC time, result from the sliding-average subtraction process, but after the SC the relations between the B, D, and I pulsations are clear. The second positive pulse in B at 1618 UT is accompanied by negative pulses in D and I, showing tailward and inward motion of the field lines. These first pulses are just the short-period (<2 min) portion of the sudden commencement.

The toroidal oscillation in D is set up immediately, with five oscillations between 1619 and 1627:30 UT. The pulsation amplitude rises until 1623 UT and then falls. A 100-s pulsation in B starts up more slowly but is clear from 1620 to 1626 UT, when B and D are in phase. The clearest correlation is

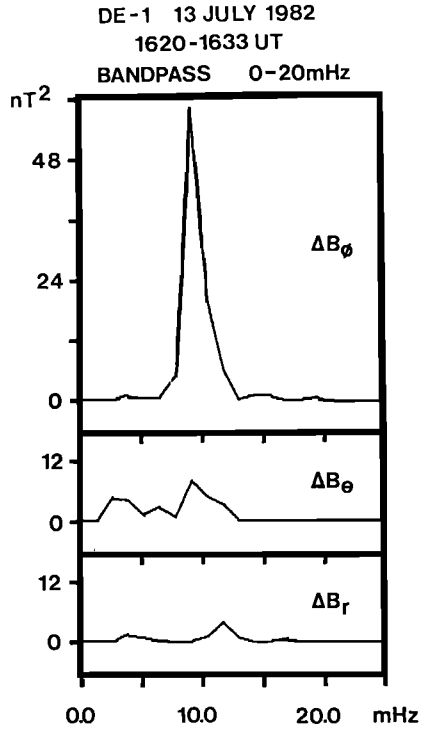

Fig. 5. Spectra of the pulsations in the interval 1620–1633 UT in B_r, B_θ, and B_ϕ components. The square of the Fourier amplitude is plotted.

seen for the three positive D and B peaks between 1621 and 1624 UT. The initial I pulsations damp rapidly by 1620 UT, but another series starts at 1621 and grows to a maximum at 1625 UT. This second set of pulsations is of shorter period than the D pulsations. Six I oscillations can be counted between 1621 and 1629 UT, giving an approximately 80-s period. Confirmation of the difference between the toroidal and poloidal periods can be seen in Figure 5. The frequency spectra of the ϕ, θ, and r components of the oscillations are shown where the ϕ, east-west, component has a sharp resonance peak near 10 mHz (100-s period). The θ, mainly compressional, component also has a 10-mHz peak as well as a peak near 3 mHz (the 300-s pulsation mentioned in the description of Figure 1). The radial, poloidal component in contrast has a peak near 11.5 mHz (87-s period). The B_θ component also has energy there. The toroidal pulsations appear to be coupled to the compressional pulsations, with a common period, but the poloidal pulsation period is slightly off. In model calculations it is shown that the resonant poloidal pulsations of a field line have a shorter period than the toroidal ones [*Cummings et al.*, 1969]. The situation here differs from the very large azimuthal wave number of Cummings' model, however. The global mode waves have small azimuthal wave number, and the compressional and poloidal modes are the same, called the fast mode for a homogeneous plasma. Once the global modes become standing waves, the location of the nodes of B_θ ($B_\parallel$) and B_r varies with frequency, so the frequency spectra need not coincide.

Poloidal pulsations, I or B_r (and also B_θ when off the equator), are confined to the magnetic meridian plane. They are associated with east-west electric field oscillations and radial He^+ ion oscillations. Figure 6 shows a phase comparison between I, E_z (east-west), and RL, the inward-outward

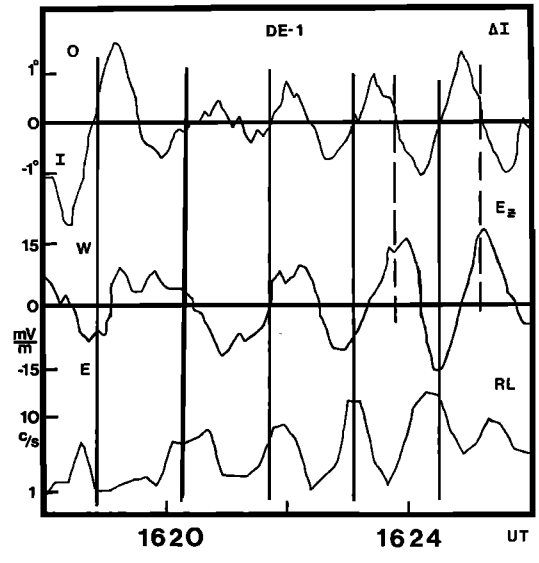

Fig. 6. A comparison of the phases of I (which shows directional changes of the B field in the magnetic meridian plane), of E_z (fluctuations of the east-west component of E), and of RL (counts of He^+ received in the radial RIMS detector when it was looking earthward). The vertical line at 1624:30 UT marks a time when the relative phases are as expected for a poloidal pulsation.

He^+ ion motion from the RIMS radial plasma head. The He^+ ion counts collected between 45° and 180° spin phase angle (outward and upward moving ions) during each radial head rotation are summed to produce RL in this figure. The maximum outward radial motion is expected as the field line passes from inward deflection to outward, $-I$ to $+I$. The solid vertical lines show that this is approximately satisfied between 1620 and 1625 UT. The electric field should also be at maximum eastward when the outward ion motion is greatest. This condition is satisfied only near 1623 and 1624:30 UT. It is puzzling why electric field oscillations disagree with the magnetic field and ion motion before 1623 UT. The reason for the discrepancy between E_z and I is because the E_z pulsations are near 100-s period while those of I are near 90 s. The E_z-I agreement near 1624 UT is a temporary phase correlation between pulsations of dissimilar period.

The E_z, east-west, electric field pulsation fits better with B, as is evident in Figure 7. There are two observations that stand out in this figure. First, B and E_z are in phase from the

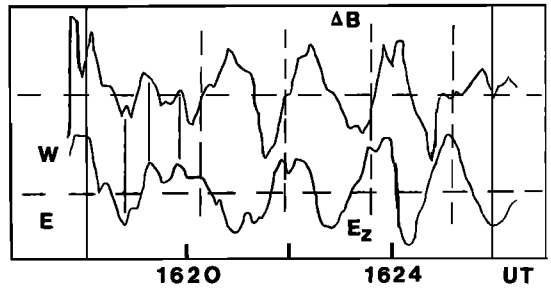

Fig. 7. A comparison of the phases of B and E_z. The dashed vertical lines between 1620 and 1624 UT mark times when the relative phases between B and E_z are as expected for compressional standing waves.

sudden commencement at 1617:30 until about 1620 UT. The phase relation, westward E_z with coincident B maxima, is appropriate for the Poynting vector of inward traveling compressional pulses. Even some minor peaks, connected by vertical lines, coincide. Second, after 1620 UT the 100-s pulsations in B are accompanied by 100-s E_z pulsations, but now the phase differs by 90°. The initial inward traveling compressional impulse is transformed to a standing compressional wave.

The sudden commencement propagates as a hydromagnetic wave, traveling inward from the magnetopause. *Chen and Hasegawa* [1974] proposed that such traveling waves, associated with impulsive changes, propagate to locations where some component of their broad wave spectrum matches the local Alfven guided mode standing wave frequency and sets up a transverse resonant standing wave. Recently, *Kivelson and Southwood* [1986] suggested that global compressional eigenmodes with quantized frequencies determined by the radial structure of the magnetosphere may play an intermediate role in setting up the transverse waves. The 100- and 300-s pulsations in B seen in Figure 1 and in the spectrum of Figure 5 may be an example of such compressional waves. In this case the sudden commencement has caused cavity resonances with periods of 100 and 300 s. The 100-s compressional eigenmode couples to a toroidal resonance at $L = 4.5$ and transfers energy to the toroidal mode. The toroidal mode in turn loses energy through ionospheric losses. The 300-s eigenmode is too low in frequency to couple to a transverse standing wave at $L = 4.5$. Of course it may have coupled to a 300-s standing wave at a higher L value.

Another treatment of the cavity resonance concept is offered by *Allan et al.* [1986]. They suggest that the plasmapause has a strong effect on the cavity resonance waves. In their model calculations, second harmonic resonances of the cavity between the ionosphere and magnetopause are stronger than the fundamental. These second harmonics have electric field nodes at the plasmapause. A particular calculation for strong compressional/toroidal coupling and with the plasmapause at $L = 4$ may be appropriate to compare with the present 100-s waves. The model compressional second harmonic has its highest amplitude just outside the plasmapause, and it couples there to the fundamental field line resonance toroidal standing wave (their figures 5 and 6). In their model the damping time of the toroidal waves before damping out is controlled by choosing the ionospheric dissipation. Their model toroidal waves damp out after about 10 pulsations as ours do, indicating the dissipation factor chosen for the model was appropriate. The 300-s compressional pulsation we observe may correspond to the lower-amplitude fundamental cavity resonance of their model, although their fundamental period is larger than the second harmonic period by a factor of 2, not 3. Interpreting our observations in Figure 7 in terms of this model, DE 1 is immersed in the compressional standing wave. When E_z is westward, the B field lines are moving inward with the plasma; when E_z is eastward, lines move outward. At the plasmapause, at somewhat lower L value than DE 1, E_z and the plasma velocity have nodes. The field lines are alternately compressed or expanded as they approach and leave the node in E_z, leading to fluctuations in field magnitude B and in plasma density.

There are two discrepancies in matching our observations

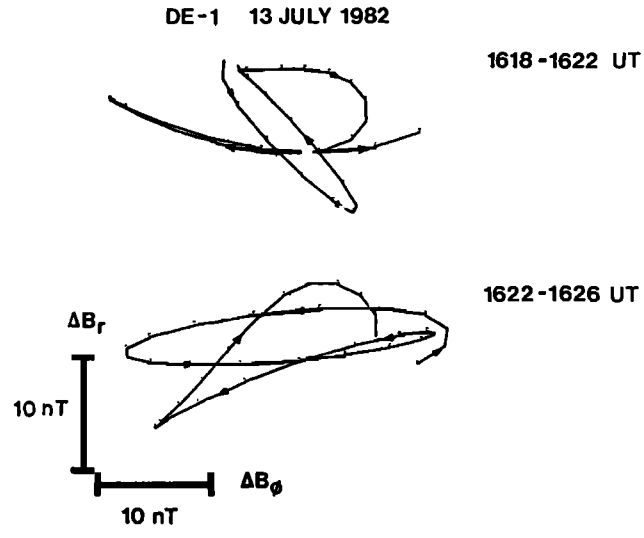

Fig. 8. Two hodogram segments showing the magnetic field perturbations of the pulsation in the B_r-B_ϕ plane.

to the global compressional/toroidal resonance models. First, the observation, in Figure 4, that D and B are in phase in the interval 1620–1626 UT is surprising. At this time the compressional waves are presumably coupled to and transferring energy to the toroidal waves. Positive B means field lines pushed inward in the compressional pulsation while positive D means lines deflected westward, toward noon from the satellite position near 1500 MLT. For the compressional/toroidal coupling we expected inward compressional motion to be accompanied by tailward toroidal motion. However, it is not so simple to predict the phase relation between B ($B_\parallel$) and D (B_ϕ) for the compressional/toroidal coupling. Maxwell's curl equations and the polarization drift formula for the perpendicular current yield

$$\frac{\partial}{\partial r_\phi} B_\parallel = \left[1 - \left(\frac{\omega}{\omega_A}\right)\right] \frac{\partial}{\partial r_\parallel} B_\phi$$

Since the toroidal waves are standing waves along the field line ($r_\parallel$), B_ϕ is in phase (or antiphase) with $(\partial/\partial r_\parallel)\, B_\phi$. This is not so for the phase relation between $B_\parallel$ and $(\partial/\partial r_\phi)\, B_\parallel$ because it is not known whether the wave is traveling or standing in the azimuthal direction. In addition, the square-bracketed expression changes sign across the exact resonance $\omega_A = \omega$. If there is damping, the toroidal eigenfrequency ω_A has an imaginary part, and the sign change occurs over a finite region as a gradual phase change from 0° to 180°. Thus, depending on where the measurements are made relative to the exact resonant field lines, almost any phase relation between B and D ($B_\parallel$ and B_ϕ) can be observed. Second, we expected the compressional amplitude to decrease while the toroidal amplitude increases, indicating the transfer of energy. The B and D pulsations in Figure 4 appear to be at peak amplitude together, from 1621 to 1624 UT. In fact the toroidal pulsations appear to be well established and growing immediately after the sudden commencement, by 1618 UT, while the compressional standing waves do not start until 1620 UT.

Another view of the initial motion of field lines after the SC is shown in Figure 8, a hodogram of the field distortions in the r-ϕ plane. The top panel starts with the magnetic field fully compressed by the SC, when B_r has its maximum positive value. This figure can be interpreted as an indication of the motion of the field lines during the SC and pulsations. Positive B_r means the field line is compressed inward, and positive B_ϕ means the field line has moved to the west. The view is from below the r-ϕ plane at the spacecraft, with west at right and in, toward the Earth, at top. After the first inward motion the field moves outward and westward and then inward and eastward, a left-hand, elliptically polarized pulsation where the toroidal and poloidal motions appear coupled. Then the two motions become uncoupled. The east-west motion continues with growing amplitude, but the radial motion decreases in amplitude, so the oscillation becomes almost linear, east-west. Dropping to the lower panel, the toroidal and poloidal motions appear to be coupled again. This left-hand, elliptically polarized oscillation (90° phase difference) of the toroidal and poloidal motion lasts for only one cycle. Finally, the toroidal and poloidal motion is out of phase again as the amplitudes of the pulsations decrease.

We have described the ULF waves, 3 mHz to 0.5 Hz, generated by the sudden commencement. Also enhanced by sudden commencements are waves in the ELF-VLF range 0.3–30 kHz [*Gail et al.*, 1990; *Gail and Inan*, 1990]. On the ground in the Antarctic, enhancements have been observed in 50% of 250 sudden commencements studied. Considering dayside events only, ELF-VLF enhancements were observed in 80% of the events. Wave changes included growth in wave amplitude, increases in upper frequency limit (where the frequency bands observed are generally below the electron gyrofrequency), and enhanced triggering of discrete emissions [*Gail et al.*, 1990]. In space, using data from the plasma wave instrument on the DE 1 spacecraft, changes in wave activity were observed in 14 of 49 sudden commencement events studied. Increases in wave amplitude and increases in upper frequency limit were observed [*Gail and Inan*, 1990]. In some cases, SC-related waves were observed above the electron gyrofrequency. One of the events in the ELF-VLF study was the July 13 sudden commencement of our report. In this case the frequency band, 2–6 kHz before the SC, shifted upward to 3–8 kHz after the SC, and waves also appeared in a band near 100 kHz. Including ULF, ELF, and VLF, this sudden commencement produced wave activity extending over 7 orders of magnitude in frequency.

It is useful to compare several published spacecraft observations of SC- or SI-related pulsations in the magnetosphere. One common feature was the occurrence of toroidal oscillations. The present DE 1 toroidal pulsations at $L = 4.5$ were of 100-s period and 10-nT amplitude, while two of the GEOS 2 observations at $L = 6.7$ showed toroidal waves at 240 s period and 2.5 mV/m amplitude [*Nopper et al.*, 1982; *Wedeken et al.*, 1986]. The Explorer 12 waves were also about 10 nT but with 250 s period [*Kaufmann and Walker*, 1974]. Table 1 provides a comparison of several features of the pulsation events. The L value, magnetic latitude, and magnetic local time of each observation are shown, as well as the amplitude of the sudden commencement, the rise time of the SC, the period and amplitude of the toroidal component, and the period of the compressional component, if any. The observation is identified with the name of the first author of the paper cited.

For the observations shown, the periods of the toroidal oscillations are mostly near 200 s, about half the period of

TABLE 1. Various Features of the Pulsation Events

Observation	L	MLAT, deg	MLT	Amplitude, nT, SC/SI	T_r, min	Toroidal Component		Compressional Component
						Period, s	Amplitude	Period, s
Kaufmann	8.2	−12	0610	40	3.0	250	10 nT	240?
Nopper	6.7	3–20	0600–1500	−5 SI	2.0	240	2.5 nT	?
Baumjohann	6.7	−3	1030	15 SI	3.0	180	0.5 mV/m	180
Wedeken	6.7	−3	1200	45	4.0	240	5 mV/m	?
Cahill	4.5	20	1520	80	3.5	100	10 nT	100, 300

the 8-min compressional pulsations observed over a large radial extent by *Kivelson et al.* [1984] and twice the period of the DE 1 observations. The global compressional modes depend mainly on the size of the cavity while the toroidal modes depend on field line length and plasma density, generally increasing in period with increasing L value. The change from 200 s to 100 s period for global oscillations implies some change in cavity size. Global resonance periods of the model are given in terms of a characteristic time, T_0 [*Allan et al.*, 1986]. For the strong coupling case with the plasmapause at $L = 4$ the resonance period is $1.02T_0$. The characteristic time is given as r_0/A_0, where r_0 is the magnetopause distance and A_0 is the Alfven velocity at the magnetopause. The magnetopause distance for the 80-nT SC is lower than for a smaller SC, perhaps as low as 7 R_E, and A_0 at the magnetopause should be higher because of higher B. A smaller characteristic time means lower global cavity resonance periods.

The DE 1 and the GEOS 2 observations by *Baumjohann et al.* [1984] show clear compressional pulsations with period matching the toroidal period. *Kaufmann and Walker* [1974] note a single compressional pulse with an estimated duration of 120 s. If we consider this pulse as one-half cycle of a rapidly damped compressional oscillation, then it suggests a compressional cavity oscillation of similar period, coupling to the 250-s toroidal oscillations. There are no visible compressional pulsations in the records of *Wedeken et al.* [1986], and such pulsations are possible but not clearly evident in the published observations of *Nopper et al.* [1982]. If compressional eigenmodes are needed to couple to resonant toroidal oscillations, then they must often be too small to observe. The question arises why the compressional pulsations are observed in the DE case and not in many others. One reason is that the coupling efficiency depends on the azimuthal wave number, m [*Allan et al.*, 1986]. For intermediate m a small compressional amplitude is sufficient, while a large or small m (as may apply here) requires a larger amplitude to excite the toroidal mode. Another reason may be the much larger SC in this case, generating a larger-amplitude compressional resonance.

In summary, small but distinct, damped (100 s) toroidal standing waves were observed at $L = 4.5$ resulting from a worldwide sudden commencement. Similar but shorter-period (90 s) poloidal waves were also seen as well as compressional pulsations of 300- and 100-s period. We suggest that the 300- and 100-s compressional pulsations are evidence of global cavity resonance oscillations and that the 100-s compressional pulsations have coupled to the toroidal and perhaps to the poloidal oscillations. The DE 1 observations were compared with other recent SC-related pulsation observations in the magnetosphere, and it was noted that toroidal oscillations occurred in each of the observations while compressional pulsations were seen less frequently.

Acknowledgments. We appreciate the assistance of the DE project office at Goddard Space Flight Center in preparing for the spacecraft mission and in the processing of data. The University of Minnesota and Augsburg College were supported by NASA through grant NAS 5-529. We acknowledge C. R. Chappell, the RIMS principal investigator, and S. D. Shawhan, the PWI principal investigator, for use of their data. The suggestions of the referees were also very helpful in improving the interpretation of the results.

The Editor thanks B. Inhester and R. Schmidt for their assistance in evaluating this paper.

REFERENCES

Allan, W., E. M. Poulter, and S. P. White, Hydromagnetic wave coupling in the magnetosphere—Plasmapause effects on impulse-excited resonances, *Planet. Space Sci.*, *34*, 1189, 1986.

Allan, W., E. M. Poulter, and S. P. White, Hydromagnetic wave coupling in the magnetosphere—Magnetic fields and Poynting fluxes, *Planet. Space Sci.*, *35*, 1181, 1987.

Baumjohann, W., H. Junginger, G. Haerendel, and O. H. Bauer, Resonant Alfven waves excited by a sudden impulse, *J. Geophys. Res.*, *89*, 2765, 1984.

Cahill, L. J., Jr., M. Sugiura, N. G. Lin, R. L. Arnoldy, S. D. Shawhan, M. J. Engebretson, and B. G. Ledley, Observation of an oscillating magnetic field shell at three locations, *J. Geophys. Res.*, *89*, 2735, 1984.

Cahill, L. J., Jr., N. G. Lin, M. J. Engebretson, D. R. Weimer, and M. Sugiura, Electric and magnetic observations of the structure of standing waves in the magnetosphere, *J. Geophys. Res.*, *91*, 8895, 1986.

Chappell, C. R., S. A. Fields, C. R. Baugher, J. H. Hoffman, W. B. Hanson, W. W. Wright, H. D. Hammack, G. R. Carignan, and A. F. Nagy, The retarding ion mass spectrometer on Dynamic Explorer-A, *Space Sci. Instrum.*, *5*, 477, 1981.

Chen, L., and A. Hasegawa, A theory of long-period magnetic pulsations, 1, Steady state excitation of field line resonance, *J. Geophys. Res.*, *79*, 1924, 1974.

Crowley, G., W. J. Hughes, and T. B. Jones, Observational evidence of cavity modes in the Earth's magnetosphere, *J. Geophys. Res.*, *92*, 12,233, 1987.

Cummings, W. D., R. J. O'Sullivan, and P. J. Coleman, Standing Alfven waves in the magnetosphere, *J. Geophys. Res.*, *74*, 778, 1969.

Engebretson, M. J., L. J. Cahill, Jr., and D. J. Williams, Pulsations in magnetic field and ion flux observed at $L = 4.5$ on August 5, 1972, *J. Geophys. Res.*, *88*, 161, 1983.

Engebretson, M. J., L. J. Zanetti, T. A. Potemra, and M. H. Acuña, Harmonically structured ULF pulsations observed by the AMPTE/CCE magnetic field experiment, *Geophys. Res. Lett.*, *13*, 905, 1986.

Farthing, W. H., M. Sugiura, B. G. Ledley, and L. J. Cahill, Jr., Magnetic field observations on the DE-A and DE-B, *Space Sci. Instrum.*, *5*, 551, 1981.

Fukunishi, H., Latitude dependence of power spectra of magnetic

pulsations near $L = 4$ excited by ssc's and si's, *J. Geophys. Res.*, *84*, 7191, 1979.

Gail, W. B., and U. S. Inan, Characteristics of wave-particle interactions during sudden commencements, 2, Spacecraft observations, *J. Geophys. Res.*, *95*, 139, 1990.

Gail, W. B., U. S. Inan, R. A. Helliwell, D. L. Carpenter, S. Krishnaswamy, T. J. Rosenberg, and L. J. Lanzerotti, Characteristics of wave-particle interactions during sudden commencements, 1, Ground-based observations, *J. Geophys. Res.*, *95*, 119, 1990.

Kaufmann, R. L., and D. N. Walker, Hydromagnetic waves excited during an ssc, *J. Geophys. Res.*, *79*, 5187, 1974.

Kivelson, M. G., and D. J. Southwood, Resonant ULF waves: A new interpretation, *Geophys. Res. Lett.*, *12*, 49, 1985.

Kivelson, M. G., and D. J. Southwood, Coupling of global magnetosphere MHD eigenmodes to field line resonances, *J. Geophys. Res.*, *91*, 4345, 1986.

Kivelson, M. G., J. Etcheto, and J. G. Trotignon, Global compressional oscillations of the terrestrial magnetosphere: The evidence and a model, *J. Geophys. Res.*, *89*, 9851, 1984.

Langel, R. A., R. H. Estes, G. Mead, E. B. Fabiano, and E. Lancaster, Initial geomagnetic field model from Magsat vector data, *Geophys. Res. Lett.*, *7*, 793, 1980.

Lezniak, T. W., and J. R. Winckler, Structure of the magnetopause at 6.6 R_E in terms of 50- to 150-keV electrons, *J. Geophys. Res.*, *73*, 5733, 1968.

Lin, N. G., L. J. Cahill, Jr., M. J. Engebretson, M. Sugiura, and R. L. Arnoldy, Dayside pulsation events near the plasmapause, *Planet. Space Sci.*, *34*, 155, 1986.

Mead, G. D., Deformation of the geomagnetic field by the solar wind, *J. Geophys. Res.*, *69*, 1181, 1964.

Mead, G. D., and L. J. Cahill, Jr., Explorer 12 measurements of the distortion of the geomagnetic field by the solar wind, *J. Geophys. Res.*, *72*, 2737, 1967.

Nopper, R. W., W. J. Hughes, C. G. McLennan, and R. L. McPherron, Impulse-excited pulsations during the July 29, 1977, event, *J. Geophys. Res.*, *87*, 5911, 1982.

Shawhan, S. D., D. A. Gurnett, D. L. Odem, R. A. Helliwell, and C. G. Park, The plasma wave and quasi-static electric field instrument (PWI) for Dynamic Explorer-A, *Space Sci. Instrum.*, *5*, 535, 1981.

Southwood, D. J., Some features of field line resonances in the magnetosphere, *Planet. Space Sci.*, *22*, 483, 1974.

Sugiura, M., A sudden change in the solar wind pressure and the outer region of the magnetosphere, *J. Geophys. Res.*, *70*, 4151. 1965.

Takahashi, K., L. M. Kistler, T. A. Potemra, R. W. McEntire, and L. J. Zanetti, Magnetospheric ULF waves observed during the major magnetosphere compression of November 1, 1984, *J. Geophys. Res.*, *93*, 14,369, 1988.

Waite, J. H., D. L. Gallagher, M. O. Chandler, R. C. Olsen, R. H. Comfort, T. F. E. Johnson, C. R. Chappell, W. L. Peterson, D. Weimer, and S. R. Shawhan, Plasma and field observations of a Pc 5 wave event, *J. Geophys. Res.*, *91*, 11,147, 1986.

Wedeken, U., H. Voelker, K. Knott, and M. Lester, SSC-excited pulsations recorded near noon on GEOS 2 and on the ground (CDAW 6), *J. Geophys. Res.*, *91*, 3089, 1986.

L. J. Cahill, Jr., Space Science Center, University of Minnesota, 100 Union Street, S.E., Minneapolis, MN 55455.

M. J. Engebretson and N. G. Lin, Physics Department, Augsburg College, Minneapolis, MN 55454.

M. Sugiura, Geophysical Institute, Kyoto University, Kyoto 606, Japan.

J. H. Waite, Jr., Department of Space Physics, Southwest Research Institute, 3500 Culebra Road, San Antonio, TX 78284.

(Received March 3, 1989;
revised December 27, 1989;
accepted December 29, 1989.)